Journal of the European Ceramic Society 20 (2000) 1319–1325

Effect of extended annealing cycles on the thermal conductivity of AlN/Y_2O_3 ceramics

Giuseppe Pezzotti[a,*], Atsushi Nakahira[a], Masahiko Tajika[b,1]

[a]*Department of Materials, Kyoto Institute of Technology, Sakyo-ku, Matsugasaki, Kyoto 606-8585, Japan*
[b]*Synergy Ceramics Laboratory, Fine Ceramics Research Association, 2-4-1, Mutsuno, Atsuta-ku, Nagoya, Aichi 456-8587, Japan*

Received 10 May 1999; received in revised form 25 October 1999; accepted 31 October 1999

Abstract

The effect of extended annealing cycles (up to 50 h at 1800°C) on the thermal conductivity of polycrystalline AlN, doped with 5 wt% Y_2O_3, has been studied. The microstructural evolution upon annealing has also been characterized in detail, using quantitative scanning electron microscopy (SEM) observation and energy dispersive X-ray analysis (EDX). As-sintered AlN/Y_2O_3 composites typically contained a dilute yttrium aluminate secondary phase well distributed and completely wetting the AlN grains. Upon annealing, the AlN matrix grains isotropically grew, while the grain-boundary yttrium aluminate phase tended to segregate to triple grain junctions. This segregation process produced a collapse of the grain-boundary film thickness, thus resulting in a completely different AlN microstructure dispersed with isolated yttrium aluminate grains. Equilibrium of the microstructural morphology was achieved after annealing times in the interval 5–10 h. As a consequence of microstructural changes, the thermal conductivity of the annealed AlN polycrystal exceeded that of the as-sintered material. A discussion is given about the variation of thermal properties in terms of both segregation to the triple-grain junctions of the intergranular Y_2O_3-phase and grain-growth of the bulk AlN grains.

Keywords: AlN-Y_2O_3; Annealing; Grain boundaries; Microstructure-final; Thermal conductivity

1. Introduction

A typical feature in ceramic processing is the addition of a limited fraction of sintering additives, typically oxides, to promote densification. However, an associated disadvantage is that non-negligible alterations may occur of the bulk property for which the ceramic phase has been originally selected.

The thermal conductivity of polyphase ceramics is strongly affected by internal phase geometry and other microstructural details.[1,2] High thermal conductivity constitutes an attractive property of AlN ceramics for high-power semiconductor devices.[3,4] However, the usual preparation of dense polycrystalline AlN bodies involves the additive Y_2O_3 which, by virtue of its good wettability of the AlN grain surface, enables ready densification by pressureless sintering.[5–7]

In this paper, we first study the microstructural evolution occurring upon extended annealing cycles (performed in nitrogen atmosphere) in a dense polycrystalline AlN with 5 wt% Y_2O_3 additive. Image analysis characterizations on SEM micrographs and EDX microanalysis are employed to reveal and to quantify the microstructural features critical for thermal properties. Finally, a theoretical discussion is given based on literature models of thermal properties in composite materials.

2. Experimental procedures

AlN powder (XUS35560, The Dow Chemical Co., Midland, MI, USA), produced by carbothermal reduction method, contained high-purity Y_2O_3 in a composition ratio 95:5, by weight (96.72:3.28, by volume). The AlN powder, with average grain size 0.5 μm, contained 0.85 wt% oxygen as a major impurity. In addition, carbon was present to a fraction 0.03 wt%, with very minor additional cation impurities (Fe, 32 ppm; Ca, 44 ppm). The specific surface area of the AlN powder was

* Corresponding author. Fax: +81-75-724-7580.
E-mail address: pezzotti@chem.kit.ac.jp (G. Pezzotti).
[1] Present address: Dow Chemical International Ltd., 92-2 Ogurano, Gotemba 412, Japan.

0955-2219/00/$ - see front matter
PII: S0955-2219(99)00286-1

2.66 m^2/g. The powder was preformed by uniaxial pressing (under ≈30 MPa) as small disks with diameter and thickness of 20 and 5 mm, respectively, followed by a cold isostatic pressing cycle (⩽300 MPa). After placing the specimens in a BN crucible, sintering was performed at 1850°C for 1 h, in a flowing nitrogen atmosphere. The heating rate was 10°C/min. The polycrystalline specimens reached a density >99%. Successive annealing cycles were performed using the same equipment of the sintered samples at 1800°C for durations of up to 50 h.

X-ray diffraction patterns by Cu-$K_{\alpha 1}$ radiation were obtained on finely crushed pieces of sintered bodies. The scanning speed was 3°/min and the diffractometer device was calibrated by standard silicon powder.

Microstructures were analyzed by a field-emission SEM (S-800, Hitachi Ltd., Tokyo, Japan) equipped with an EDX device. Image analysis data of grain size, grain-boundary thickness and triple-point size were collected on polished surfaces, according to the circle intercept method proposed by Hilliard and Cahn.[8] The surface area quantitatively scanned by image analysis was ≈0.1 mm^2 for each material.

Thermal conductivity was measured according to the laser-flash method, using a 5J CO_2 laser. The measurement device was supplied with a non-contact infrared detector and a computer-controlled data acquisition system. Data were averaged on three measurements for each material.

3. Results

3.1. Microstructural characterization

Microstructures of the AlN/3.28 vol%–Y_2O_3 materials were observed by SEM on polished surfaces both in the as-sintered state (1 h at 1850°C) [Fig. 1(A)], and after annealing for 5, 10, 20, 30, 50 h at 1850°C [Figs. 1(B),(C),(D),(E),(F), respectively]. In the as-sintered specimen, fine AlN matrix grains were rounded and continuously encompassed by an Y_2O_3 phase, which obviously acted as the wetting liquid during sintering. A twofold effect was found for the annealing cycle on the overall microstructural morphology: (i) the AlN matrix grains showed significant isotropic grain growth; and, (ii) the morphological arrangement of the intergranular Y_2O_3-based phase gradually changed from the geometry of a continuous wetting film toward that of a dispersion of isolated grains trapped at triple junctions of the AlN matrix. This segregation phenomenon, which involves the collapse of the intergranular film thickness in favour of an enlargement of triple-grain junctions, is better envisaged in the higher magnification SEM images of Fig. 2. Besides, isotropic grain growth occurred, AlN grains also lost their rounded morphology and became well facetted. This phenomenon suggests the occurrence of a change in the ratio of interfacial energy between the grains and the liquid phase. This phenomenon was already observed by previous investigators.[9] Quantitative plots of the AlN (average) grain size, intergranular film thickness and triple-point size of the segregated Y_2O_3 phase are shown in Fig. 3(A),(B) and (C), respectively. As seen, all these morphological parameters showed a somewhat abrupt change for annealing times in the interval between 5 and 10 h. On the other hand, their respective variations obeyed a rather saturated dependence on time for annealing duration longer than ≈10 h. In other words, the microstructure of the present AlN/Y_2O_3 system seems to reach sufficient thermodynamic stability after annealing times at least longer than 10 h (at 1800°C). The average thickness of the intergranular film after >10 h became undetectable under the maximum magnification allowed by our field-emission SEM device. Thus, we shall assume that such a thickness, if any, should experience a nanometre-scale magnitude after long-term annealing. Migration of liquid matter toward triple-grain junction resulted in a saturated size of Y_2O_3 isolated grains of ≈3 μm. The presence of such Y_2O_3 grains may have delayed further grain growth in the AlN matrix. Nevertheless, measurements of areal fraction by the systematic point-counting method[10] showed that the fraction of the secondary phase did not appreciably vary upon annealing.

In order to detect eventual changes in phase composition upon sintering/annealing, EDX experiments were conducted on materials in the as-sintered state and after 50 h annealing at 1800°C. The results of the EDX experiments are summarized in Fig. 4. Elemental maps of Y and O reveal the intragranular presence of both these elements in the AlN matrix, meaning that a reciprocal exchange of ions has actually occurred between the AlN and Y_2O_3 phases during heat treatment. Al ions were also detected within the intergranular phase. Thus, a dilute solid solution in the Y–Al–O–N system has formed in the AlN grains, concurrently with the formation of a yttrium silicate phase to replace Y_2O_3 at grain boundaries. However, although this diffusion phenomenon may have triggered wettability between grains and liquid, concentrations of Y and O species within the AlN grains is not pronounced. In addition, diffusion does not appear to be significantly enhanced by the annealing time. Similar amounts of Y and O (≈0.4 and 1.5 at%, respectively) were detected within the AlN grains either after 1 h sintering at 1850°C or further 50 h annealing at 1800°C.

3.2. Thermal conductivity characterization

Fig. 5 shows the dependence of thermal conductivity on the annealing time at elevated temperature. As a general trend, thermal conductivity increased with increasing the annealing time. Compared with the as-sintered

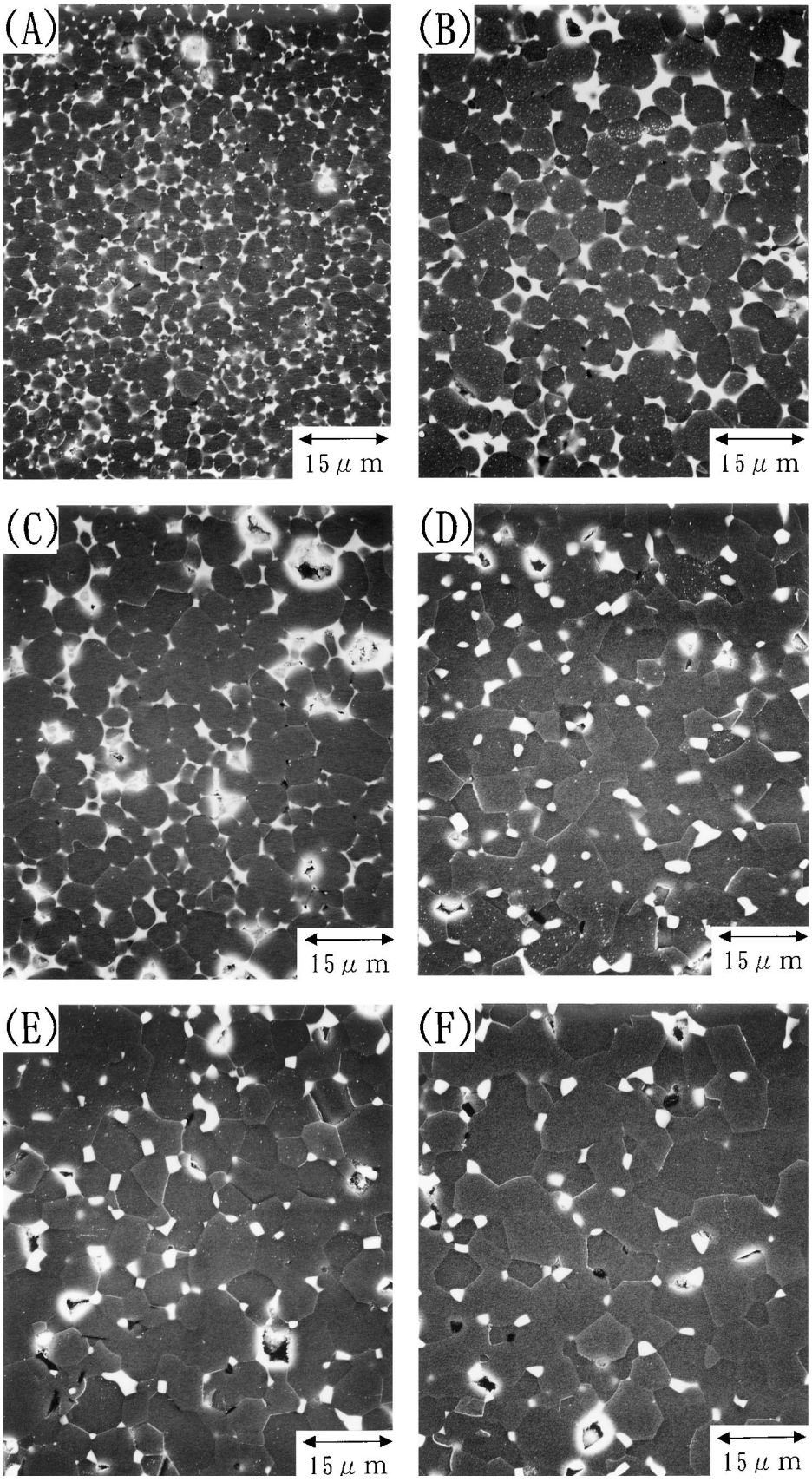

Fig. 1. Microstructures of the AIN/5 wt%-Y_2O_3 material observed by SEM on randomly cut and polished surfaces: material in the as-sintered state (1 h at 1850°C) (A), and after annealing for 5, 10, 20, 30, 50 h at 1800°C [(B),(C),(D),(E),(F), respectively].

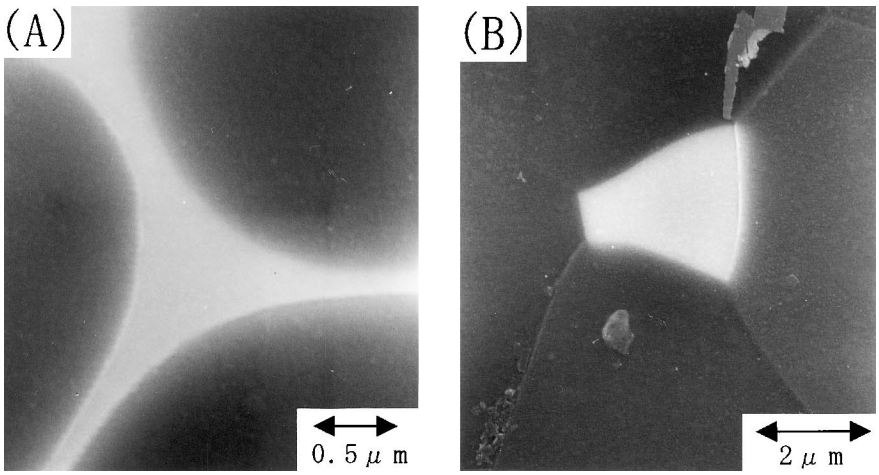

Fig. 2. Higher magnification SEM images of grain boundary in as-sintered (A) and 50 h annealed (B) samples. Both the grain-boundary phase migration toward triple-grain junctions and the facetting of the AlN grains are clearly envisaged.

material, the materials annealed for times >10 h showed consistently higher thermal conductivity values, the maximum improvement being of about 25%. An important implication can be found in the plot of Fig. 5, in comparison with the microstructural features summarized in Fig. 3. The increase of thermal conductivity appears to follow the same trend as the microstructural changes, namely an abrupt change between 5 and 10 h annealing. In other words, the migration of the grain-boundary phase from the intergranular film toward the triple points seems to be the most important process affecting the thermal properties of the present ceramic system. Depleted grain-boundary thickness ultimately reaches an equilibrium state in which a large number of AlN grains are facetted and directly bonded to each other, thus producing the closest thermal performance to a bulk AlN polycrystal.

In the present context, the formation of solid solutions are regarded as having only a secondary effect on the thermal conductivity of the present ceramic system. However, the concentration of Y and O at grain boundaries are not markedly enhanced even after 50 h annealing, despite an appreciable variation of thermal conductivity is found after annealing for times >10 h.

4. Discussion

4.1. Intrinsic thermal conductivity of bulk AlN grains

A dominant impurity of the AlN powder is oxygen, which has been shown to play an important role on the intrinsic thermal conductivity of AlN ceramic.[11] Upon sintering, the oxygen enters the AlN lattice and can substitute for the nitrogen up to very high oxygen concentrations.[12] In this process, one molecule of $Al_{0.67}O$ substitutes for one molecule of AlN. Since the tetrahedral covalent radius of oxygen is less than that of nitrogen,[13] and since metal vacancies occur on the aluminum sites, the AlN lattice parameter should decrease as the oxygen content increases. This has been indeed verified experimentally in the present material after a long-term annealing cycle, where the c-axis lattice parameter was determined by X-ray diffraction analysis as $c = 4.9795$ Å (with a standard deviation < 0.0003 Å), against the lattice parameter of a highly pure AlN, reported as $c_0 = 4.9816$ Å.[14] The lattice constant measured in the as-sintered material did not significantly differ from the value found in the annealed material. This implies that the Y_2O_3 phase was rather stable at high temperature, in agreement with the EDX data described in Section. 3.1

Slack[14] has precisely determined the relation between the c-axis parameter and the oxygen concentration in the AlN lattice. A linear relationship was found to hold in a wide range of solid solutions, up to high oxygen concentrations:

$$\Delta c/c_0 = -0.021(\Delta n/n_0) \quad (1)$$

where n_0 is the number of nitrogen atoms per unit volume in pure AlN (i.e., 4.79×10^{28} m^{-3}), Δn is the number of nitrogen atoms that have been replaced by oxygen, and Δc is the change in c-axis lattice parameter caused by Δn. In addition, the incremental thermal resistivity caused by the soluted oxygen was also found to obey the linear law:

$$\Delta W/\Delta n = 0.90 \times 10^{-29} m^4 K/W \quad (2)$$

From Eqs. (1) and (2) and using the lattice parameter determined by X-ray diffraction, the parameter $\Delta W = W - W_0 \approx 1.23$ m K/W can be calculated for the present material. Then, assuming the thermal resistivity of nominally pure AlN as $W_0 = 1/320$ m K/W[14], a value of $K_m = 1/W = 230$ W/m K is found for the thermal conductivity of the bulk Al–O–N grains in the present

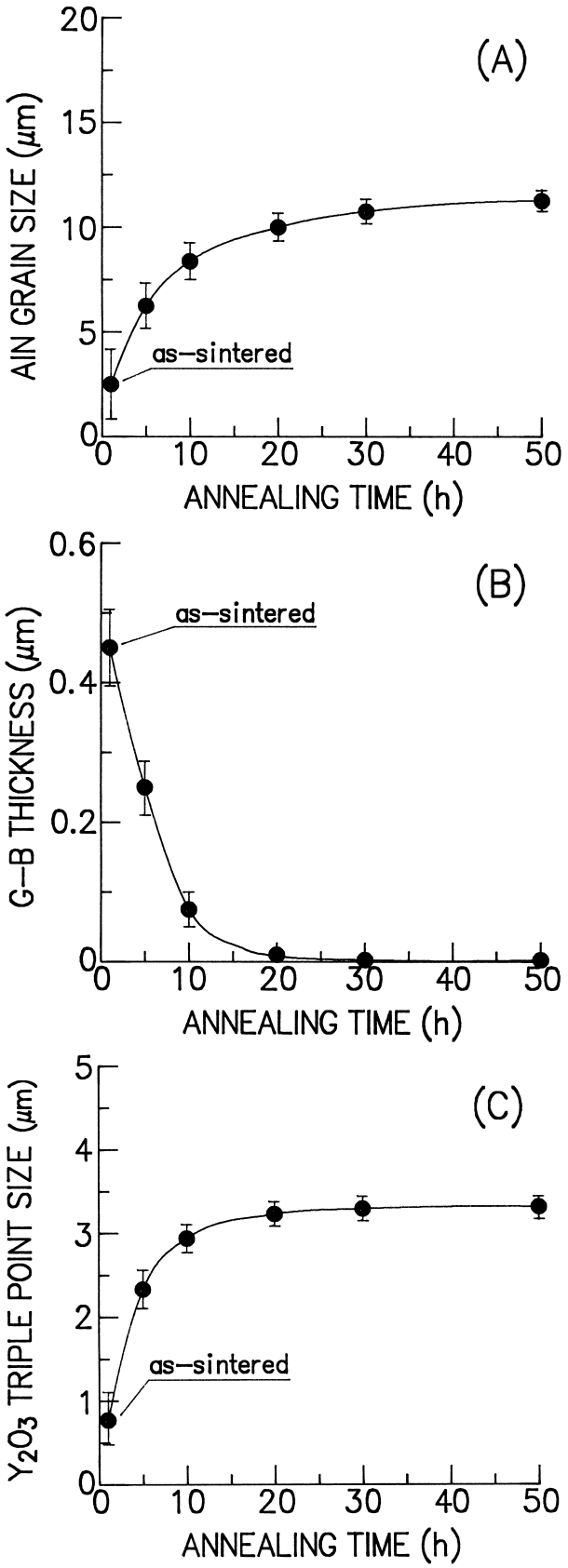

Fig. 3. Plots of AlN (average) grain size (A), intergranular film thickness (B) and size of Y_2O_3 particles located at triple points (C), as obtained by quantitative image analysis on SEM micrographs. Error bars represent the standard deviations of the respective measurements.

polycrystalline system. This value will be used in the following in an attempt to discuss the effect of intergranular Y_2O_3 on the thermal conductivity of AlN.

4.2. Thermal conductivity of AlN after long-term annealing

The microstructure developed after long-term annealing is that of a composite material whose matrix (AlN) is dispersed with a low fraction of particles (Y_2O_3) of lower thermal conductivity.

Many models of thermal conductivity have been proposed for composite materials, which attempt to predict the concurrent effect of morphology, volume fraction and intrinsic thermal conductivity of a secondary dispersed phase. A model by Nielsen[15] is followed here which, despite its relatively simple formulation, applies over a wide range of the above constituent parameters. According to Nielsen's model the thermal conductivity of a composite material, K_c, is related to that of the matrix, K_m according to the following equation:

$$K_c = K_m[(1 + ABV_f)/|1 - B\beta V_f|] \quad (3)$$

where

$$B = [(K_f/K_m - 1)/(K_f/K_m + A)] \quad (4)$$

$$\beta = 1 + [(1 - V_M)/V_M^2]V_f \quad (5)$$

in which K_f and V_f are the thermal conductivity and the volume fraction of the secondary added phase, respectively, V_M is the maximum packing fraction of the added phase and A is an adimensional shape factor which depends on the geometry of the particles. A is related to the generalized Einstein coefficient, published for a number of solid and liquid suspensions with various characteristics.[15] V_M has been calculated as 0.637 for irregular random-close particles,[15] while the A value is bound between 1.5 and 2, values rigorously valid for spheres and cubes, respectively.[15,16] Note that the Nielsen's model completely neglects the effect of grain size on thermal conductivity. In addition, for $A \rightarrow \infty$ and $V_M = 1$, Eq. (3) reduces to the simple rule of mixture:

$$K_c = V_f K_f + (1 - V_f)K_m \quad (6)$$

Predictions for the thermal conductivity of the AlN/Y_2O_3 composite after long-term annealing are shown in Fig. 5. They are based both on the Nielsen's model [Eqs. (3)–(5)] and on the rule of mixture [Eq. (6)] for the present ceramic system. In the calculation, we assumed $K_f = 60.7$ W/m K and $K_m = 230$ W/m K, for polycrystalline Y_2O_3[17] and AlN phases (see Section 4.1), respectively. Given the rather low volume fraction of

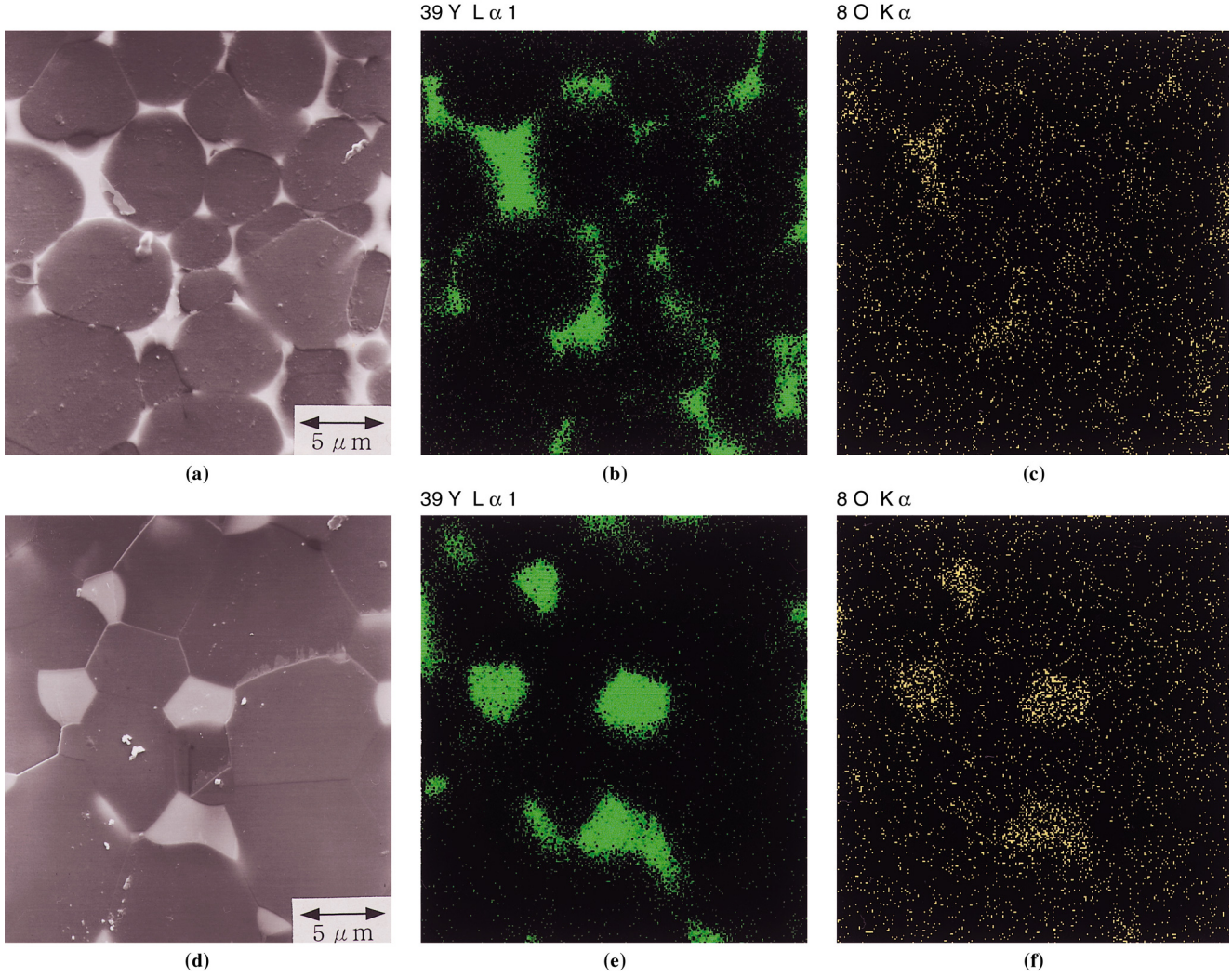

Fig. 4. SEM images and elemental maps of Y and O in the as-sintered material [(A)–(C)] and after 50 h annealing [(D)–(F)]. In both cases, the elemental maps reveal traces of both Y and O into the AlN matrix grains, which means that ion exchange promptly occurs (and saturates) upon heat treatment within the AlN and Y_2O_3 phases.

the dispersed Y_2O_3 phase, the predictions by both the models are very close to each other and both enable to justify the measured thermal conductivity after long-term annealing in the present composite.

4.3. Thermal conductivity of the as-sintered AlN

In Section 4.2, a homogeneous and continuous AlN medium containing a fraction of isolated and randomly dispersed Y_2O_3 particles has been selected to represent the case of the AlN/Y_2O_3 ceramic after long-term annealing cycle. In that case, Y_2O_3 was regarded as the dispersed phase in the AlN matrix, and the thermal conductivity of the composite experienced an upper value.

A lower bound for thermal conductivity of the present ceramic system can be calculated for the material in the as-sintered state. In this case, the Y_2O_3 phase is considered to be the matrix phase, despite its low volume fraction. This model is justified by the morphology of Y_2O_3 being that of a continuous film which separates (nearly) spherical AlN grains. The AlN grains, despite their high volume fraction, are thus regarded as the dispersed phase.

According to this microstructural model, a lower bound for thermal conductivity can be again calculated from Eqs. (3) to (6). In the calculation, the shape factor $A = 0.5$ is taken which is adequate for microstructures with elongated features whose direction is transverse to the heat flow.[15] The maximum packing fraction of the AlN grains should lie in the interval $0.524 < V_M < 0.60$, whose lower and upper limits are the values calculated for dispersed spheres with simple-cubic and body-centred cubic packing order, respectively.[15] The experimental value of thermal conductivity $K_c = 178$ W/m K can indeed be predicted by taking $V_M = 0.565$. This lower limit for thermal conductivity is also plotted in Fig. 5. As for the morphology of the experimental curve in Fig. 5, its steep rising within the narrow annealing

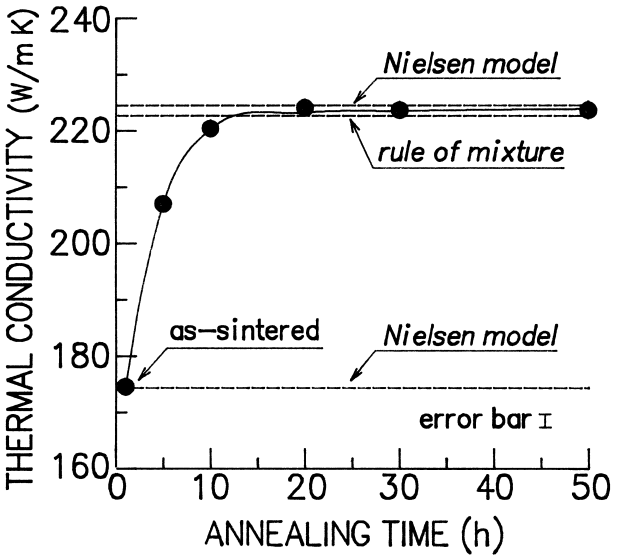

Fig. 5. Dependence of thermal conductivity on the annealing time at 1800°C. The error bar represents the maximum scatter detected among three different measurements. Predictions of thermal conductivity based on the Nielsen's model[15,16] [Eqs. (3)–(6)] are compared with the experimental data.

interval 5–10 h suggests that the number of depleted (i.e. directly bonded) AlN grain boundaries governs the transient thermal behavior of the material. However, adequate models for describing thermal conductivity in composite materials whose secondary phase maintains a constant volume fraction, but changes its morphology, are not presently available. A theoretical model which can appropriately describe the transient thermal behavior of the present AlN/Y_2O_3 material is presented in a separate paper. [18]

5. Conclusion

The effect of extended annealing cycles on thermal conductivity of AlN/Y_2O_3 ceramics has been investigated. It has been shown that the details of the microstructural arrangement can be varied upon annealing and play an important role in the thermal performance of this polycrystalline system. A phenomenon of intergranular diffusion has been found according to which annealing alters the internal geometry of the secondary Y_2O_3 phase. After sintering for 1 h at 1850°C, the secondary Y_2O_3 phase is present with the morphology of a continuous film circumventing micrometre size, rounded AlN grains. Upon annealing at 1800°C, mass migration occurs of the Y_2O_3 phase toward the triple junctions. Concurrently, AlN grains grow and become facetted, the Y_2O_3 phase assuming the final morphology of a dispersion of isolated particles with irregular shape. This mass-transport phenomenon is completed for annealing times >10 h, after which the ceramic system is thermodynamically stable, and further AlN grain growth is hampered by the micrometre-sized Y_2O_3 grains. Long-term annealed specimens showed a thermal conductivity 25% higher than that of the as-sintered specimen, due to the achieved discontinuous geometry of the low conducting Y_2O_3 phase. Thermal conductivity data are discussed according to a theoretical model given by Nielsen for polymer-matrix composites. According to this discussion, the grain-boundary migration phenomenon is regarded as a main factor determining the thermal conductivity behavior of the composite. The effect of solid solution of oxygen in the bulk AlN grains is also examined and its role on the thermal response of the material clarified.

Acknowledgements

The authors sincerely thank Mr. K. Horibe for helping in the experimental work.

References

1. Progelhof, R. C., Throne, J. L. and Ruetsch, R. R., *Polym. Eng. Sci.*, 1976, **16**, 615–621.
2. Ott, H. J., *Plastic Rubber Process. Appl.*, 1981, **1**, 9–14 .
3. Werdecker, W. and Aldinger, F., *IEEE Trans. C.H.M.T.*, 1984, **7**, 399–404.
4. Sheppard, L. M., *Am. Ceram. Soc. Bull.*, 1990, **69**, 1801–1815.
5. Komeya, K., Inoue, H. and Tsuge, A., *Yogyo-Kyokai-shi*, 1981, **89**, 330–333.
6. Kuramoto, N., Taniguchi, H., Numata, Y. and Aso, I., *Yogyo-Kyokai-shi*, 1985, **93**, 517–521.
7. Kurokawa, Y., Utsumi, K. and Takamizawa, H., *J. Am. Ceram. Soc.*, 1988, **71**, 588–593.
8. Hilliard, J. E. and Cahn, J. W., *Trans. AIME*, 1961, **221**, 344–348.
9. Virkar, A. V., Jackson, T. B. and Cutler, R. A., *J. Am. Ceram. Soc.*, 1989, **72**, 2031–2235.
10. Underwood, E. E., *Quantitative Stereology*. Addison-Wesley, Reading, MA, 1970.
11. Adams, I., AuCoin, T. R. and Wolff, G. A, *J. Electrochem. Soc.*, 1962, **109**, 1050–1056.
12. Borom, M. P., Slack, G. A. and Szymaszek, J. W., *Ceramic Bulletin*, 1972, **51**, 852–858.
13. Pauling, L., *The Nature of the Chemical Bond. 3rd edn*. Cornell University Press, Ithaca, New York, 1960.
14. Slack, G. A., *J. Phys. Chem. Solids*, 1973, **34**, 321–330.
15. Nielsen, L. E., *Ind. Eng. Chem. Fundam.*, 1984, **13**, 17–28.
16. Nielsen, L. E., *J. Appl. Polym. Sci.*, 1973, **17**, 3819–3825.
17. *Ceramic Source*, The American Ceramic Society, Westerville (OH), 1985.
18. Pezzotti, G., *J. Ceram. Soc. Japan*, 1999, **107**, 944–948.